DOI:
10.1152/physiolgenomics.00139.2017

Document Version
Peer reviewed version

Title: Sugar sensor genes in the murine gastrointestinal tract display a cephalocaudal axis of expression and a diurnal rhythm

Authors: Patrick O'Brien [1], Rhys Hewett [1], Christopher Corpe [1*]

Affiliations: [1]Department of Nutritional Sciences, School of Medicine, King's College London

Room 3.114, Franklin-Wilkins Building, 150 Stamford Street, London, SE1 9NH, United Kingdom

*Corresponding author: Christopher Corpe

Department of Nutritional Sciences, School of Medicine, King's College London, Room 3.114, Franklin-Wilkins Building, 150 Stamford Street, London, SE1 9NH

Tel: 0(44) 2078484269

Fax: 0(44) 2078484169

Email: christopher.corpe@kcl.ac.uk

"The authors have declared that no conflict of interest exists

Abstract

Distributed along the length of the gastrointestinal (GI) tract are nutrient sensing cells that release numerous signalling peptides influencing GI function, nutrient homeostasis and energy balance. Recent studies have shown a diurnal rhythm in GI nutrient sensing, but the mechanisms responsible for rhythmicity are poorly understood. In this report we studied murine GI sugar sensor gene and protein expression levels in the morning (7am) and evening (7pm). Sweet taste receptor (*tas1r2/tas1r3/gnat3/ gnat1*) sugar transporter (*slc5a1, slc2a2, slc2a5*) and putative sugar sensor (*slc5a4a and slc5a4b*) gene expression levels were highest in tongue, proximal and distal small intestine, respectively. Clock gene (*cry2/arntl*) activity was detected in all regions studied. *Slc5a4a* and *slc5a4b* gene expression showed clear diurnal rhythmicity in the small intestine and stomach, respectively, although no rhythmicity was detected in SGLT3 protein expression. *Tas1r2* and *tas1r3, gnat1* and *gcg* displayed a limited rhythm in gene expression in proximal small intestine. Microarray analysis revealed a diurnal rhythm in gut peptide gene expression in tongue (7am vs 7pm) and *in silico* promoter analysis indicated intestinal sugar sensors and transporters possessed the canonical E box elements necessary for clock gene control over gene transcription. In this report we present evidence of a diurnal rhythm in genes that are responsible for intestinal nutrient sensing that is most likely controlled by clock gene activity. Disturbances in clock gene/nutrient sensing interactions may be important in the development of diet-related diseases, such as obesity and diabetes.

Introduction

The GI tract is responsible for nutrient assimilation and determining the nutritional quality of ingested food and it achieves this via the coordinated expression of nutrient sensors, digesters and transporters. Assimilation of dietary carbohydrates begins in the mouth with salivary amylase breaking down starch into a range of molecular fragments , including alpha limit dextrin, maltose and maltotrioses (40). In tongue taste receptors cells (TRCs) the sweet taste receptor, T1R2/3, and the intracellular signalling molecule αGustducin (and possibly transducin) mediate simple sugar taste perception via increased intracellular Ca^{2+} and activation of the gustatory nerve (32). Amylase, maltase-glucoamylase (MGAM) sucrase-isomaltase (SI) glucose transporters (SGLT1, GLUT2, 4, 8 and 9) and incretins (GIP/GLP1) have recently been detected in rodent TRCs and are thought to mediate the sixth taste of complex carbohydrates and cephalic responses, including insulin release (13, 42, 47) and possibly gut motility and secretion. Carbohydrate digestion ceases in the stomach but carbohydrate sensing may still occur because T1R3 has been detected in ghrelin positive cells (17). Carbohydrate breakdown continues in the small intestine due to the activities of amylase secreted by the pancreas into the intestinal lumen and the disaccharidases (MGAM and SI) expressed on the brush border membrane of enterocytes (40). Transport of simple sugars such as glucose and fructose from the intestinal lumen into portal circulation is mediated by brush border SGLT1 and GLUT5 and basolateral GLUT2 (10). T1R2/3 and αGustducin have been detected in duodenal L-cells and play a role in the long term regulation of small intestinal glucose transport capacity via the regulation of SGLT1 gene and protein expression levels in neighbouring enterocytes (6, 19, 28). T1R2/3 and αGustducin have also been detected in rodent jejunal enterocytes and play a role in the short term regulation of small intestinal sugar transport capacity via insertion of GLUT2 into the apical membrane of enterocytes (25). SGLT1 has also been detected in enteroendocrine cells and may also act as an intestinal sugar sensor (14). GLUT5, has also been detected in GLUTag cells, a well-established *in vitro* model of the L cell; furthermore, although fructose

promotes GLP-1 release *in vitro* (15) the role of GLUT5 as an *in vivo* sugar sensor remains unclear. SGLT3 is a putative sugar sensor expressed in the myenteric plexus of the GI tract as well as a number of other tissues such as the hypothalamus, portal vein, skeletal muscle and kidney (3, 39). Mice null for the SGLT3 gene do not display a phenotype (M. Fukazawa, ADA 2013) and so the biological importance of SGLT3 remains unknown.

Previous studies have shown a diurnal rhythm in sweet taste perception (31) carbohydrate digestion (16) sugar transport capacity (2) and in GLP1 secretory response to nutrients (12); however, the molecular mechanisms responsible for the observed rhythmicity remain poorly understood. In rodents, small intestinal sugar transporter gene and protein expression levels are at a nadir in the early hrs of the morning (3am-9am) and reach a zenith in the first few hrs of the dark cycle (6pm-9pm) (7) that is dependent on clock gene activity (33). Clock genes (e.g *arntl, cry2 and per1*) control many physiologic processes, and therefore, may regulate the expression of the intestinal nutrient sensor gene expression levels. In this report we used rodents to study diurnal rhythms in the expression patterns of the sugar sensor genes along the length of the GI tract.

Materials and methods

Animals

All procedures were carried out according to the project license guidelines under the UK Home Office Animals Scientific Procedures Act, 1986. CD-1 and C57BL/6J male mice were obtained from Charles River, UK, Manston Road, Margate, CT9 4LT, Kent, England. Male CD-1 and C57BL/6 mice were kept under standard conditions with free access to standard chow and water. A standard 12-hour dark/light cycle with the start of the light cycle at 6am and the start of the dark cycle at 6pm was under automatic regulation. 6-week-old CD-1 mice and 11-week-old C57BL/6 mice were randomly divided into two groups (7am and 7pm) before being euthanized by cervical dislocation whilst under halothane anaesthesia. 7am mice (n= 16: 8 CD-1 and 8 C57BL/6 mice) were euthanised between 6 and 7am, whilst 7pm mice (n=16: 8 CD-1 and 8 C57BL/6 mice) were euthanized between 6 and 7pm and whole tongue, a segment of the stomach body and small intestinal tissues removed. For duodenum, a 2-3 cm intestinal segment 2cm distal to the stomach's pylorus was removed. For jejunum, the ligament of Trietz was identified and 2-3 cm of mid-jejunum removed. For ileum, a 2-3 cm intestinal segment was removed 5 cm proximal to the large intestine. Tissues were dissected into tubes and immediately snap-frozen in liquid nitrogen for further RNA and protein extraction.

RNA extraction

Tissue was incubated overnight in RNAlater®-ICE solution (Life Technologies, USA) at-20°C. 15 mg of tissue was then homegenized in Qiazol (Qiagen) in a Qiagen TissueLyser for 3x30 s at 30 Hz, and RNA extracted using an RNeasy Lipid Tissue Mini Procedure (Qiagen, Netherlands), following the manufacturer's protocol.

Reverse Transcription Polymerase Chain Reaction (RT-PCR)

1 µg of RNA was reverse transcribed with a High capacity RNA-to-cDNA kit (Applied Biosystems, USA) according to the manufacturer's protocol in a PTC-200 Peltier Thermal cycler. The resulting cDNA was diluted 1:10 in water, and PCR performed using 10 ng cDNA and a primer concentration of 900nM with FastStart Universal Probe Master (ROX) (Roche, Switzerland) mastermix. PCR conditions: using an AB 7000 qPCR cycler (Applied Biosystems, USA), 10 min at 95°C for polymerase activation, 40 cycles of 95°C annealing for 15 s and 1 min at 60°C for amplification. Primers were designed using Roche's online ProbeFinder Software, ver. 2.50. The mouse genome was selected to design PCR assays over exon-exon borders for transcriptome specificity. All primers were obtained from IDT (Leuven, Belgium) and reconstituted with ultrapure water to a stock concentration of 10 µM. *18s* 5'-gcaattattccccatgaacg-3' and 5'gggacttaatcaacgcaagc-3'(UPL#48); *hprt1* 5'-tcctcctcagaccgctttt-3' and 5'-cctggttcatcatcgctaatc-3' (95); *hmbs* 5'- tccctgaaggatgtgcctac-3' and 5'-aagggttttcccgtttgc-3'(79); *slc5a1* 5'-ctggcaggccgaagtatg-3' and 5'-ttccaatgttactggcaaagag-3'(49); *slc2a2* 5'-gggccatcaacatgatcttc-3' and 5'-aatcatcccggttaggaaca-3' (70); *slc2a5* 5'-agagcaacgatggaggaaaa-3' and 5'-ccagagcaaggaccaatgtc-3'(94); *slc5a4a*5'-aaacccattcccgatgttc-3' and5'-tcgattctttcctccttactgttc-3'(107); *slc5a4b* 5'-ccgattcctgatgttcacct-3' and 5'-atccgctcctctgtgttgtt-3'(67); *gcg* 5'-cacgcccttcaagacacag-3' and 5'-gtcctcatgcgcttctgtc-3' (33); *cck* 5'-tgatttccccatccaaagc-3' and 5'-gcttctgcagggactaccg-3'(9); *gip* 5'caggtaggaggagaagacctcat-3' and 5'-cctagattgtgtcccctagcc-3'(79); *ghrl* 5'-ccagaggacagaggacaagc-3' and 5'-catcgaagggagcattgaac-3'(17); *arntl1* 5'-tacagtggccctttgcatct-3' and 5'cccaaattcccacatctga-3' (47); *cry2* 5'-ccgcctgtgggacttgta-3' and 5'-ctccattcggtcaaacctg-3'(49); *gnat3* 5'-tccaaagaactggagaagaagc-3' and 5'-tttcccagattcacctgctc-3'(88); *gnat1* 5'-agagctggagaagaagctgaaa-3' and 5'-tagtgctcttcccggattca-3'(89); *tas1r1* 5'-gggcctgataacactgacca-3' and 5'-tgctcgcctcatagctgac-3'(74). For relative quantification, the ddCT method was performed using the reference genes *18s, hprt1* and *hmbs* for normalisation.

QuantiFast® tas1r2 & tas1r3 real-time PCR

As we were not successful in quantifying expression of *tas1r2* and *tas1r3* using UPL primers designed assays, we used QuantiFast® Probe Assay kits (Qiagen) with predesigned primers and probes - tas1r2 (Cat. No: QF00096929) and tas1r3 (Cat. No: QF00030016) and followed the manufacturer's manual. PCRs were performed on an AB 7000 qPCR cycler (Applied Biosystems, USA).

Microarray analysis

400 ng of RNA was pooled from tongue tissue obtained at 7am and 7pm and integrity confirmed on an Agilent Bioanalyzer chip. RNA was labelled with a GeneChip® 3' IVT Express Kit (Affymetrix, USA) and analysed using a GeneChip MouseGenome 430A 2.0 Array following the manufacturer's instructions. Data was analysed using the GeneGo software (MetaCore™, version 6.19 build 65960 - Thomson Reuters).

Protein extraction

15 mg of tissue was dissected on dry ice and homogenised in ice-cold protein-extraction buffer (1mM fresh DTT, 50mM Tris-HCl pH 7.4, 250mM Mannitol, 100mM NaCl, 1mM EDTA, 1mM EGTA, 10% glycerol) containing 1x protease-inhibitor cocktail (Sigma-Aldrich P8340, Dorset/UK) using a Qiagen TissueLyser for 2x60s at 30 Hz. Samples were then incubated on a rotating spinner for 30min at 4°C and then centrifuged at 13,000 RPM for 10 min at 4°C. The protein-containing supernatant was transferred into a new tube. Protein content was quantified using a Pierce™ BCA Protein assay kit.

Western blotting

Protein lysates were made up at a final concentration of 5 µg/µl, including 4x NuPAGE® LDS sample buffer (Life Technologies) and 10x sample-reducing agent (Life Technologies). Samples were then heated

for 5 min at 95°C and 20 µg were loaded onto a 4-12% gradient NuPAGE Bis-Tris Protein gels. Proteins were separated for 55 min at 200 V in an XCell sure-lock tank with 1x NuPAGE® MOPS SDS running buffer (Life Technologies). The Western transfer was then performed using a Bio-Rad TurboBlot in cold Transfer buffer (25mM Tris-base, 75 mM Glycine, 10% Methanol, 0.1% SDS) and a 0.45 µm Immobilon-P PVDF membrane (Merck Millipore, Cork/IRL). Proteins were transferred for 90 min at 20V with a 100 mA cut-off. PVDF membranes were blocked in 5% milk powder in TBS+Tween 0.1% (TBST) for 1 h. Blots were rinsed 3x and washed for 3x 5 min in TBST. Primary antibodies (1:2000) in TBST with 0.05% Sodium Azide and blots were incubated over-night at 4°C. Antibodies were from Santa Cruz Biotechnology, Heidelberg/DE: βActin sc-130656, GLUT2 sc-31826, SGLT3 sc-134521. Blots were rinsed 3x and washed for 3x 5 min in TBST and blocked for 10 min. Anti-rabbit secondary antibody (sc-2004) (1:2000) in blocking buffer and blots were incubated for 1 h at room temperature. Blots were rinsed 3x, washed for 3x 10 min in TBST and incubated for 3 mins with ECL Prime (GE Healthcare, Little Chalfont/UK). Protein signal was visualised using a SynGene G:BOX with the GeneSnap software, version 7.12 (Synaptics, Cambridge/UK) and a 1-20 min exposure time.

In silico promotor analysis

To obtain 10,000bp of sequence upstream of the transcription start sites of the sugar sensor, transporter and gut peptide genes, we undertook a gene specific promoter scan of the mouse genome (mouse: Dec. 2011 (GRCm38/mm10) using the genome browser at UCSC. E-Box elements within each promoter were then retrieved manually in Microsoft Word.

Statistics

Data analysis and statistics were performed using Excel included in Microsoft Office Pro 2007, Version 12.0.6661.5000 SP3 MSO. Data are given as arithmetic mean + standard deviation (SD). Significances

were tested using the inbuilt two-sided T-Test of Excel. A P-value of 0.05 or less was considered statistically significant.

Study approval.

The procedures included in this manuscript were approved by the appropriate Committees on the Use and Care of Animals at King's college London.

196 Results

197 To assess the expression levels of genes associated with sugar sensing in the GI tract we isolated tongue,
198 stomach, duodenum, jejunum and ileum from CD-1 mice at 7 am and 7 pm and by qPCR measured
199 mRNA levels of *tas1r1* (T1R1), *tas1r2* (T1R2), *tas1r3* (T1R3), *gnat1* (TRANSDUCIN), *gnat3* (αGUSTDUCIN),
200 *slc5a4a* (SGLT3a), *slc5a4b* (SGLT3b), *slc5a1* (SGLT1), *slc2a2* (GLUT2), *slc2a5* (GLUT5), and peptides, *ghrl*
201 (GHRELIN) *cck* (CCK) *gcg* (PREPROGLUCAGON) and *gip* (GIP).

202 Consistent with previous reports (49) mRNA expression of *slc5a1*, *slc2a2* and *slc2a5* are highest in the
203 proximal regions of the small intestine, namely the duodenum and jejunum, and lowest in the distal
204 regions, namely the ileum (Figure 1). qPCR for the sugar transporters in whole tongue and stomach
205 samples was not undertaken; however, a recent report detected *Slc5a1* and *slc2a5* gene and protein
206 expression have been detected in TRCs in mouse tongue (47).

207 Consistent with previous reports in rodents (7) sugar transporter gene expression levels were
208 dependent on time (Figure 1). In duodenum, jejunum and ileum, *slc5a1*, *slc2a2* and *slc2a5* gene
209 expression levels increased 2-4 fold between 7am and 7pm. In C57BL/6 mice, small intestinal GLUT2
210 mRNA (data not shown) and protein levels also increased significantly between the hrs of 7am and 7pm,
211 as shown by Western blot analyses of GLUT2, normalized against βActin (Figure 2). Duodenal GLUT2
212 protein expression levels increased 3- fold between 7am and 7pm, whereas in the jejunum and ileum
213 the change in protein expression levels were more modest, showing only a ~50% increase between 7am
214 and 7pm.

215 Expression levels of the umami, bitter and sweet-taste receptor genes *tas1r1*, *tas1r2* and *tas1r3* were
216 highest in the tongue: 20-45-fold higher than in duodenum at 7am (Figure 3). Contrary to data published
217 in mouse (4, 41) we were not able to detect *tas1r1* or *tas1r2* expression in the stomach. However,
218 *tas1r3* was detectable in stomach at levels of expression similar to those detected in small intestine.

Tas1r1, tas1r2 and *tas1r3* transcripts were detected in all small intestinal segments: *tas1r1* and *tas1r3* gene expression levels were highest in jejunum, whereas *tas1r2* expression levels were highest in duodenum. Expression of the genes responsible for downstream nutrient signalling, Transducin (*gnat1)* and αGustducin (*gnat3)* were highest in proximal gut (tongue and stomach) and lowest in distal gut (duodenum, jejunum and ileum) (Figure 3). When compared to duodenum at 7am, tongue *gnat1* and *gnat3* expression levels were 20- and 5-fold higher, and in stomach gnat1 and gnat3 expression levels 250- and 20- fold higher.

Expression levels of the umami, bitter and sweet-taste receptor genes *tas1r1*, *tas1r2* and *tas1r3* showed some evidence of time dependency (Figure 3); however, the direction of the change in expression levels was inconsistent between segments, the fold changes were modest (0.3-2.5-fold) and they did not always reach statistical significance. In tongue, *tas1r1* gene expression levels showed a small but significant increase (31%) in expression between 7am and 7pm, whereas in other intestinal segments no significant change was detected. *Tas1r2* gene expression levels in tongue and ileum was not significantly changed, whereas in the duodenum and jejunum there was a trend towards increased expression, with duodenal and jejunal *tas1r2* gene expression levels increasing 2-2.5-fold between 7am and 7pm. *Tas1r3* gene expression levels were unchanged in tongue, stomach and ileum, however, in duodenum expression levels increased by 40%, while in the jejunum they decreased by 25%. For *gnat1* there was a trend towards increased gene expression with time in all regions studied but none reached statistical significance. Studies using more time points throughout the day may have produced more robust data. *Gnat3* gene expression levels were unchanged overall, although in duodenum we detected a non-significant 1.5-fold increase in expression.

In mice, the putative sugar sensor SGLT3 exists in two forms: *slc5a4a* (SGLT3a) and *slc5a4b* (SGLT3b). Our analysis revealed that *slc5a4a* was not detectable in tongue or stomach (Figure 4); however, in small

intestine *slc5a4a* expression was detectable, especially in the distal regions: jejunal and ileal expression levels were 5-8 fold higher than duodenal expression at 7am. *Slc5a4b* was undetectable in tongue and barely detectable in stomach. In small intestine, however, *slc5a4b* expression levels were detectable and highest in distal regions: 4-6 fold higher in jejunum and ileum when compared to duodenum at 7am.

Slc5a4a and *slc5a4b* expression levels in small intestine showed evidence of time dependency (Figure 4). Between 7am and 7pm, *Slc5a4a* expression levels in duodenum, jejunum and ileum were increased 6-fold, 2.5-fold and 3-fold, respectively, although ileal data did not reach statistical significance. Slc5a4b showed a 5-fold increase in the stomach, whereas in the small intestine no significant change in expression was detected. To determine if the detected changes in SGLT3 transcript levels resulted in changes in SGLT3 protein expression levels we performed Western Blot on protein obtained from C57BL/6 mice isolated from the stomach, duodenum jejunum and ileum at 7am and 7pm. *Slc5a4a* and *sl5a4b* gene expression was altered similarly to those detected in CD1 mice (data not shown); however, no change in SGLT3 protein expression levels were detected in any of the intestinal regions studied (Figure 5).

Cck gene expression levels were similar along the length of the small intestine (Figure 6), whereas *gip* expression was approx. 4-fold higher in duodenum, when compared to jejunum and ileum, and *gcg* expression (preproglucagon is translated and cleaved into GLP1 and GLP2) was 15-fold higher in ileum, when compared to duodenum an ileum. qPCR for gut peptides in whole tongue and stomach tissue was not undertaken; however, a recent report have detected *gcg*/GLP1 positive staining in isolated TRC from mouse tongue (42).

To assess the time dependency of gut peptide gene expression levels, we measured *ghrl* gene expression levels in stomach, and *cck*, *gip*, *gcg* in small intestine at 7am and 7pm. *Ghrl* levels in stomach were unchanged between 7 am and 7pm (Figure 6). *Cck* and *gip* gene expression levels were not time

dependent in all intestinal segments studied (Figure 6). However, between 7am and 7pm, *gcg* gene expression levels showed a non-significant increase (85%) in the duodenum and a significant increase (43%) in the jejunum, no change in ileal *gcg* expression levels were detected.

The canonical clock genes, *cry2* and *arntl1* were expressed in all intestinal regions studied (Figure 7). However, *cry2* gene expression levels were highest in the tongue: 4.5-fold above those detected in duodenum at 7am, whereas *arntl1* expression was lowest in the stomach: 5-fold below duodenum at 7am. Expression levels of *cry2* and *arntl1* were also time dependent (Figure 7). Between 7am and 7pm *cry2* gene expression levels significantly increased between 0.5-3-fold in all intestinal regions studied, except for the stomach, which showed a non-significant decrease of 50%. Between 7am and 7pm, *arntl1* showed a significant 7-fold decrease in gene expression levels in all intestinal regions.

Recent findings have shown that many of the known gut peptides, such as GLP1, Ghrelin and CCK can also be detected in lingual taste buds (18, 37). Because clock genes were active in tongue tissue we decided to undertake microarray analysis of pooled tongue tissue collected at 7 am and 7pm. Array data showed the expression of *gcg, pyy, ghrl* and *cck* was downregulated from 7am to 7pm, whereas *gip* expression was upregulated (Table 1).

Clock genes (e.g. CRY2, BMAL1) can regulate gene expression by binding to the promotor, or, within or downstream of the transcript. Clock genes regulate target genes by binding to E-Box cis-regulatory enhancer sequences, and it has been suggested that clock genes bind not only the canonical E-Box sequence used by all basic Helix-Loop-Helix transcription factors but also an extended E-Box sequence of the form (G/T)G(A/G)ACACGTGACCC (51). To determine the presence of such extended E-Box elements in the intestinal sugar sensors and transporter genes we undertook an *in silico* analysis of their promoter regions. Within 10,000bp upstream of their transcription-initiation sites we found the canonical E-Box sequence CACGTG in all genes apart from *cry2*, *gip* and *gcg* (Table 2). Analysing these sequences for the

extended E-Box sequence, we found a near perfect fit for *arntl1*/BMAL1 and *slc2a2*/GLUT2 (matches highlighted in bold). *Slc5a1*/SGLT1, *tas1r1*/T1R1, *tas1r2*/T1R2, *tas1r3*/T1R3, *slc5a4a*/SGLT3a, *slc5a4b*/SGLT3b, *ghrl*/ghrelin, *cck*/cck and *pyy*/PYY have at least two nucleotide matches. Several intronic E-Boxes were found for *cry2*. Directly beside each other are two E-Boxes, with one of them having a high match to the extended circadian E-Box sequence; 15,115bp and 15,168bp downstream of the first exon the sequences TGTG-CACGTG-AGCC and CTGC-CACGTG-CCAG were found. These data suggest intestinal nutrient sensors are subject to clock gene control.

Discussion

The GI tract tightly regulates nutrient assimilation in order to protect the organism from ingesting harmful substances, efficiently deliver nutrients to metabolically active tissues and to prevent nutrient malabsorption. A number of intestinal processes display a diurnal rhythm that are subject to clock gene control; however, there is limited information on mechanisms responsible for the diurnal rhythm in intestinal nutrient sensing. In this report we have assessed the gene expression patterns of the sugar sensors in tongue, stomach and small intestine and have found evidence of a diurnal rhythm that may be subject to clock gene control.

Sugar sensing on the tongue is mediated by the sweet taste receptor T1R2/3 and the intracellular signalling molecule αGustducin (24). The sweet taste machinery is expressed in the taste cells of fungiform papillae located in the anterior part of the tongue and is activated by simple sugars and artificial sweeteners (AS). T1R2/3 is also expressed in the circumvallate papillae located in the posterior part of the tongue; however αGustducin does not co-localize (21) suggesting the presence of another intracellular signalling molecule, possibly transducin (35) or Gα14 subunit (38). Upon activation by sugars and AS, tongue T1R2/3 appears to drive motivation to ingest sugar (hedonics, palatability and reward). It is noteworthy that although deletion of T1R2 and T1R3 genes impact on the motivation to ingest simple sugars, the ability to detect and respond to more complex carbohydrates persists (23, 45) indicating the presence of a T1r2/3 independent carbohydrate sensing mechanism. *Slc5a4a and 4b* was not detected in murine tongue tissue, suggesting SGLT3 plays no role in sugar sensing in taste receptor cells. T1R2 or T1R3 alone may be responsible. In addition, expression of amylase, disaccharidases (SI and MGAM) and sugar transporters (SGLT1, GLUT2 and GLUT5) have been detected in taste receptor cells and it was suggested that activation of this sixth taste pathway by complex carbohydrates plays a role in the cephalic insulin response (30, 42, 47).

Prior to the onset of feeding, the orexigenic hormone ghrelin is synthesized by the X/A cells in the oxyntic glands of the stomach and released in increasing quantities into the blood (48). Once feeding is initiated, circulating ghrelin levels rapidly decline. It is unclear if the decline in ghrelin's release is a pre- or post-absorptive signalling event and the molecular identity of the nutrient sensing mechanism(s) in stomach has yet to be established. In agreement with another report (4) we did not detect *tas1r2* in stomach tissue, suggesting the heterodimeric sweet taste receptor, T1R2/3, does not act as a stomach sugar sensor. The sugar transporters, GLUT2 and SGLT1 and αGustducin also do not appear to be involved in stomach sugar sensing (41). Consistent with another report (17) we detected *tas1r3* and *gant3* expression in stomach as well as *gant1*. Indeed, *gant1* and *gant3* expression levels were highest in stomach when compared to other segments of the GI tract. T1R3 is activated when sucrose levels are between 300-500mM, suggesting T1R3 may function as a low affinity sucrose sensor (50). In rodent studies, daily exposure to sucrose impairs central dopaminergic food cue learning, possibly via a dysregulation in ghrelin signalling (36). Although speculative, disturbances in stomach sucrose sensing mediated by T1R3/ghrelin release may provide a mechanistic explanation for the epidemiologic data that has indicated an association between consumption of sugar sweetened beverages and poor metabolic health (26). Knockout mice in which T1R3 has been conditionally deleted in stomach could be used to test this possibility.

We also detected the expression of *slc5a4b* (but not *slc5a4a*) and SGLT3 protein in stomach. Although the SGLT3 antibody does not distinguish between SGLT3 a and b isoforms we assume only SGLT3b is expressed in mouse stomach, most likely in myenteric and submucosal cholinergic neurons (39). Mouse SGLT3b transports glucose poorly but will elicit a membrane depolarizing current (H^+ and Na^+) at both acidic and neutral pH (3). Human SGLT3 doesn't transport sugar, but produces a membrane depolarization in response to glucose but not fructose (8). Collectively, these data suggest SGLT3b in

rodents (and SGLT3 in humans) act as a stomach glucose sensor and may explain why glucose (but not fructose) is a potent suppressor of ghrelin's release (44).

The final stages of nutrient digestion and absorption occur in the small intestine. As digestion and transport progresses along the length of the small intestine luminal levels of sugars decrease and there is a concomitant reduction in small intestinal sugar digestive/transport capacity, which is reflected by the cephalocaudal axis of sugar transport gene and protein expression levels presented in this report and by others (49). T1R2/3 and αGustducin expressed in the small intestine regulate intestinal sugar transport capacity in response to short and long term changes in dietary carbohydrate levels (25, 28) but their expression levels in all segments of the small intestine were similar, suggesting the sweet taste receptor machinery itself is not regulated by luminal levels of dietary sugar.

Slc4a4a and *slc4a4b* transcripts and SGLT3 protein were also detected in small intestine, with gene expression highest in jejunum and ileum, suggesting SGLT3 is not positively regulated by luminal levels of dietary sugar levels. SGLT3b appears to most highly expressed in ileum and if it does function as a glucose sensor, then it may play a role in the negative feedback loop ("the ileal brake"), which controls gastric motility and emptying (27). When glucose binds to SGLT3a a membrane depolarization occurs under acidic (pH 5) but not neutral conditions (pH 7.4) (1). SGLT3a may therefore act as a mid-intestinal sugar sensor activated when acidic chyme is ejected from the stomach. Whole body and conditional SGLT3 knockout studies could further elucidate the biological importance of this putative sugar sensor.

Rodents are nocturnal feeders and consume about 80% of their daily calories during the first few hours of the dark cycle (9). Previous studies in humans have shown a diurnal rhythm in sweet taste sensitivity which is modulated by circulating leptin levels (31). Although we detected clock gene activity in tongue tissue by qPCR we found no evidence of a diurnal rhythm in *tas1r1, 2* or *3*, *gant1* or *gant3* gene expression. In addition, in our pooled tongue sample array data, no rhythmicity was detected in the

gene responsible for the so called sixth taste sensing pathway of complex carbohydrates (mediated via amylase, MGAM, SI and glucose transporters). These data indicate diurnal rhythms in sweet taste sensitivity are not due to rhythmicity in sugar sensor expression levels, which might be desirable as this would allow for an accurate assessment of ingested nutrients at all times. *Gcg, pyy, ghrl* and *cck* gene expression levels were however downregulated (2-3 fold) between 7am and 7pm, whereas GIP gene expression was increased 2-fold. GLP-1 receptor (GLP-1R) knockout studies suggest GLP1 release from taste cells influences neural and behavioural responses to sugar (43). Rhythmicity in taste responses may instead be due to leptin regulating the expression levels of gut peptides in taste cells, which in turn could influence the levels of gut peptides released during meal ingestion.

A diurnal rhythmicity in ghrelin's release from the stomach has been shown to be under the control of clock genes (BMAL1/ARNTL) (22). Moreover, food entrains both clock and ghrelin expression levels in ghrelinoma cells, suggesting a food-entrainable oscillator (FEO) system may reside in ghrelin releasing cells. Despite clock gene activity being detected in the stomach, *ghrelin, tas1r3, gnat3* and *gnat1* gene expression levels were unchanged between 7am and 7pm. We did however detect a robust diurnal rhythm in *slc5a4b* expression in stomach, suggesting stomach SGLT3 is under clock gene control. Interestingly, SGLT3 protein did not display a diurnal rhythm. Rhythmicity in gene but not protein expression (and vice versa) is in fact quite common and due to diurnal translational or posttranslational processing resulting in changes in protein half-life (29). The biological significance of these data is however currently unclear. Disruption in clock genes and SGLT3 could be a potential route to uncover the role of the SGLT3 in the stomach. Future proteomic and transcriptomic studies using isolated cells would also shed further light on the rhythmicity in intestinal nutrient sensors.

Coincident with peak levels of carbohydrate in the small intestinal lumen during the first few hours of the dark cycle, intestinal sugar transporter genes, proteins and transport capacity reaches their zenith

(7). This anticipatory rise in intestinal sugar transporter expression levels and activity during the daytime is synchronised by clock genes (34) and ensures nutrient transport capacity is matched to luminal nutrient load. There is also some evidence that small intestinal nutrient sensing mechanisms display a diurnal rhythm. Diurnal rhythms in the GLP1 secretory response have been previously reported in rodent and humans (11) and in GLUT-ag cells secretion of the incretin GLP1 has been shown to be under the control of clock genes (12). We have also recently detected clock genes expressed in STC1 cells, a well-established *in vitro* model of the K cell, and in NCI-NH76 cells, a well-established *in vitro* model of human enteroendocrine cells (unpublished data). In this report, we show evidence of a modest diurnal rhythm in the gene expression levels of *gcg, tas1r2* and *3* and *gnat3* in duodenum and jejunum, but not in ileum. Together these data suggest small intestinal enteroendocrine cells possess a rhythmicity synchronized by clock genes.

We have shown in this report evidence the genes responsible for intestinal nutrient sensing display a cephalocaudal axis of expression and a diurnal rhythm. Diurnal rhythms are synchronized by clock genes and studies have shown SNPs in clock genes are associated with increased risk of metabolic disease (46). In support, mice null for the clock gene develop obesity and metabolic syndrome along with hyperphagia, hyperlipidemia (elevation of triglycerides and cholesterol) hyperglycemia, hyperleptinemia and hypoinsulinemia (20). Disturbances in clock gene activity could therefore lead to disturbances in intestinal nutrients sensing contributing towards metabolic disease. In addition, shift workers are at increased risk of developing GI disturbances and metabolic disease (5) which could be due to disturbances in the synchronization of clock genes by the FEO and Light-entrainable oscillator system (LEO) systems Although the LEO system is well characterized the molecular identity of the FEO remains obscure. We speculate the nutrient sensors described herein as well as protein, fat and umami sensors play a role in synchronizing intestinal clock genes and that phasic synchrony of central and peripheral tissue clocks brings about necessary patterns of behavior and physiology to allow metabolic wellbeing.

When it is considered that metabolic conditions represent a huge burden on healthcare then a better understanding of their underlying mechanisms may have the potential of leading to significant therapeutic advances.

Author contributions

Christopher Corpe: Study design, Experimental work (tissue isolations), preparation of manuscript.

Patrick O'Brien: Study design, Experimental work (tissue isolation, micro array studies, qPCR, Western blotting), data analysis, preparation of manuscript.

Rhys Hewett: Experimental work (qPCR), preparation of manuscript.

Acknowledgements:

This work was supported by the Kings college studentship fund. We are also grateful for the assistance of Prof. V. Preedy and Dr. L. Brooks in tissue extraction.

447 References

448 1. **Aljure O, and Diez-Sampedro A**. Functional characterization of mouse sodium/glucose
449 transporter type 3b. *American journal of physiology Cell physiology* 299: C58-65, 2010.
450 2. **Balakrishnan A, Tavakkolizadeh A, and Rhoads DB**. Circadian clock genes and implications for
451 intestinal nutrient uptake. *The Journal of nutritional biochemistry* 23: 417-422, 2012.
452 3. **Barcelona S, Menegaz D, and Diez-Sampedro A**. Mouse SGLT3a generates proton-activated
453 currents but does not transport sugar. *American journal of physiology Cell physiology* 302: C1073-1082,
454 2012.
455 4. **Bezencon C, le Coutre J, and Damak S**. Taste-signaling proteins are coexpressed in solitary
456 intestinal epithelial cells. *Chemical senses* 32: 41-49, 2007.
457 5. **Brum MC, Filho FF, Schnorr CC, Bottega GB, and Rodrigues TC**. Shift work and its association
458 with metabolic disorders. *Diabetology & metabolic syndrome* 7: 45, 2015.
459 6. **Cheeseman CI**. Upregulation of SGLT-1 transport activity in rat jejunum induced by GLP-2
460 infusion in vivo. *The American journal of physiology* 273: R1965-1971, 1997.
461 7. **Corpe CP, and Burant CF**. Hexose transporter expression in rat small intestine: effect of diet on
462 diurnal variations. *The American journal of physiology* 271: G211-216, 1996.
463 8. **Diez-Sampedro A, Hirayama BA, Osswald C, Gorboulev V, Baumgarten K, Volk C, Wright EM,**
464 **and Koepsell H**. A glucose sensor hiding in a family of transporters. *Proceedings of the National*
465 *Academy of Sciences of the United States of America* 100: 11753-11758, 2003.
466 9. **Ellacott KL, Morton GJ, Woods SC, Tso P, and Schwartz MW**. Assessment of feeding behavior in
467 laboratory mice. *Cell metabolism* 12: 10-17, 2010.
468 10. **Ferraris RP, and Diamond J**. Regulation of intestinal sugar transport. *Physiological reviews* 77:
469 257-302, 1997.
470 11. **Gil-Lozano M, Hunter PM, Behan LA, Gladanac B, Casper RF, and Brubaker PL**. Short-term sleep
471 deprivation with nocturnal light exposure alters time-dependent glucagon-like peptide-1 and insulin
472 secretion in male volunteers. *American journal of physiology Endocrinology and metabolism* 310: E41-50,
473 2016.
474 12. **Gil-Lozano M, Mingomataj EL, Wu WK, Ridout SA, and Brubaker PL**. Circadian secretion of the
475 intestinal hormone GLP-1 by the rodent L cell. *Diabetes* 63: 3674-3685, 2014.
476 13. **Glendinning JI, Stano S, Holter M, Azenkot T, Goldman O, Margolskee RF, Vasselli JR, and**
477 **Sclafani A**. Sugar-induced cephalic-phase insulin release is mediated by a T1r2+T1r3-independent taste
478 transduction pathway in mice. *American journal of physiology Regulatory, integrative and comparative*
479 *physiology* 309: R552-560, 2015.
480 14. **Gorboulev V, Schurmann A, Vallon V, Kipp H, Jaschke A, Klessen D, Friedrich A, Scherneck S,**
481 **Rieg T, Cunard R, Veyhl-Wichmann M, Srinivasan A, Balen D, Breljak D, Rexhepaj R, Parker HE, Gribble**
482 **FM, Reimann F, Lang F, Wiese S, Sabolic I, Sendtner M, and Koepsell H**. Na(+)-D-glucose cotransporter
483 SGLT1 is pivotal for intestinal glucose absorption and glucose-dependent incretin secretion. *Diabetes* 61:
484 187-196, 2012.
485 15. **Gribble FM, Williams L, Simpson AK, and Reimann F**. A novel glucose-sensing mechanism
486 contributing to glucagon-like peptide-1 secretion from the GLUTag cell line. *Diabetes* 52: 1147-1154,
487 2003.
488 16. **Hara E, and Saito M**. Diurnal change in digestion and absorption of sucrose in vivo in rats.
489 *Journal of nutritional science and vitaminology* 35: 667-671, 1989.
490 17. **Hass N, Schwarzenbacher K, and Breer H**. T1R3 is expressed in brush cells and ghrelin-producing
491 cells of murine stomach. *Cell and tissue research* 339: 493-504, 2010.

18. **Herness S, Zhao FL, Lu SG, Kaya N, and Shen T**. Expression and physiological actions of cholecystokinin in rat taste receptor cells. *The Journal of neuroscience : the official journal of the Society for Neuroscience* 22: 10018-10029, 2002.
19. **Jang HJ, Kokrashvili Z, Theodorakis MJ, Carlson OD, Kim BJ, Zhou J, Kim HH, Xu X, Chan SL, Juhaszova M, Bernier M, Mosinger B, Margolskee RF, and Egan JM**. Gut-expressed gustducin and taste receptors regulate secretion of glucagon-like peptide-1. *Proceedings of the National Academy of Sciences of the United States of America* 104: 15069-15074, 2007.
20. **Johnston JD, Ordovas JM, Scheer FA, and Turek FW**. Circadian Rhythms, Metabolism, and Chrononutrition in Rodents and Humans. *Advances in nutrition* 7: 399-406, 2016.
21. **Kim MR, Kusakabe Y, Miura H, Shindo Y, Ninomiya Y, and Hino A**. Regional expression patterns of taste receptors and gustducin in the mouse tongue. *Biochemical and biophysical research communications* 312: 500-506, 2003.
22. **Laermans J, Vancleef L, Tack J, and Depoortere I**. Role of the clock gene Bmal1 and the gastric ghrelin-secreting cell in the circadian regulation of the ghrelin-GOAT system. *Scientific reports* 5: 16748, 2015.
23. **Lapis TJ, Penner MH, and Lim J**. Humans Can Taste Glucose Oligomers Independent of the hT1R2/hT1R3 Sweet Taste Receptor. *Chemical senses* 2016.
24. **Lee AA, and Owyang C**. Sugars, Sweet Taste Receptors, and Brain Responses. *Nutrients* 9: 2017.
25. **Mace OJ, Affleck J, Patel N, and Kellett GL**. Sweet taste receptors in rat small intestine stimulate glucose absorption through apical GLUT2. *The Journal of physiology* 582: 379-392, 2007.
26. **Malik VS**. Sugar sweetened beverages and cardiometabolic health. *Curr Opin Cardiol* 32: 572-579, 2017.
27. **Maljaars PW, Peters HP, Mela DJ, and Masclee AA**. Ileal brake: a sensible food target for appetite control. A review. *Physiology & behavior* 95: 271-281, 2008.
28. **Margolskee RF, Dyer J, Kokrashvili Z, Salmon KS, Ilegems E, Daly K, Maillet EL, Ninomiya Y, Mosinger B, and Shirazi-Beechey SP**. T1R3 and gustducin in gut sense sugars to regulate expression of Na+-glucose cotransporter 1. *Proceedings of the National Academy of Sciences of the United States of America* 104: 15075-15080, 2007.
29. **Mauvoisin D, Wang J, Jouffe C, Martin E, Atger F, Waridel P, Quadroni M, Gachon F, and Naef F**. Circadian clock-dependent and -independent rhythmic proteomes implement distinct diurnal functions in mouse liver. *Proceedings of the National Academy of Sciences of the United States of America* 111: 167-172, 2014.
30. **Merigo F, Benati D, Cristofoletti M, Osculati F, and Sbarbati A**. Glucose transporters are expressed in taste receptor cells. *Journal of anatomy* 219: 243-252, 2011.
31. **Nakamura Y, Sanematsu K, Ohta R, Shirosaki S, Koyano K, Nonaka K, Shigemura N, and Ninomiya Y**. Diurnal variation of human sweet taste recognition thresholds is correlated with plasma leptin levels. *Diabetes* 57: 2661-2665, 2008.
32. **Nelson G, Hoon MA, Chandrashekar J, Zhang Y, Ryba NJ, and Zuker CS**. Mammalian sweet taste receptors. *Cell* 106: 381-390, 2001.
33. **Pan X, and Hussain MM**. Clock is important for food and circadian regulation of macronutrient absorption in mice. *Journal of lipid research* 50: 1800-1813, 2009.
34. **Rhoads DB, Rosenbaum DH, Unsal H, Isselbacher KJ, and Levitsky LL**. Circadian periodicity of intestinal Na+/glucose cotransporter 1 mRNA levels is transcriptionally regulated. *The Journal of biological chemistry* 273: 9510-9516, 1998.
35. **Sainz E, Cavenagh MM, LopezJimenez ND, Gutierrez JC, Battey JF, Northup JK, and Sullivan SL**. The G-protein coupling properties of the human sweet and amino acid taste receptors. *Developmental neurobiology* 67: 948-959, 2007.

36. **Sharpe MJ, Clemens KJ, Morris MJ, and Westbrook RF**. Daily Exposure to Sucrose Impairs Subsequent Learning About Food Cues: A Role for Alterations in Ghrelin Signaling and Dopamine D2 Receptors. *Neuropsychopharmacology : official publication of the American College of Neuropsychopharmacology* 41: 1357-1365, 2016.
37. **Shin YK, Martin B, Golden E, Dotson CD, Maudsley S, Kim W, Jang HJ, Mattson MP, Drucker DJ, Egan JM, and Munger SD**. Modulation of taste sensitivity by GLP-1 signaling. *Journal of neurochemistry* 106: 455-463, 2008.
38. **Shindo Y, Miura H, Carninci P, Kawai J, Hayashizaki Y, Ninomiya Y, Hino A, Kanda T, and Kusakabe Y**. G alpha14 is a candidate mediator of sweet/umami signal transduction in the posterior region of the mouse tongue. *Biochemical and biophysical research communications* 376: 504-508, 2008.
39. **Sotak M, Marks J, and Unwin RJ**. Putative tissue location and function of the SLC5 family member SGLT3. *Experimental physiology* 102: 5-13, 2017.
40. **Southgate DA**. Digestion and metabolism of sugars. *The American journal of clinical nutrition* 62: 203S-210S; discussion 211S, 1995.
41. **Steensels S, Vancleef L, and Depoortere I**. The Sweetener-Sensing Mechanisms of the Ghrelin Cell. *Nutrients* 8: 2016.
42. **Sukumaran SK, Yee KK, Iwata S, Kotha R, Quezada-Calvillo R, Nichols BL, Mohan S, Pinto BM, Shigemura N, Ninomiya Y, and Margolskee RF**. Taste cell-expressed alpha-glucosidase enzymes contribute to gustatory responses to disaccharides. *Proceedings of the National Academy of Sciences of the United States of America* 113: 6035-6040, 2016.
43. **Takai S, Yasumatsu K, Inoue M, Iwata S, Yoshida R, Shigemura N, Yanagawa Y, Drucker DJ, Margolskee RF, and Ninomiya Y**. Glucagon-like peptide-1 is specifically involved in sweet taste transmission. *The FASEB journal : official publication of the Federation of American Societies for Experimental Biology* 29: 2268-2280, 2015.
44. **Teff KL, Elliott SS, Tschop M, Kieffer TJ, Rader D, Heiman M, Townsend RR, Keim NL, D'Alessio D, and Havel PJ**. Dietary fructose reduces circulating insulin and leptin, attenuates postprandial suppression of ghrelin, and increases triglycerides in women. *The Journal of clinical endocrinology and metabolism* 89: 2963-2972, 2004.
45. **Treesukosol Y, and Spector AC**. Orosensory detection of sucrose, maltose, and glucose is severely impaired in mice lacking T1R2 or T1R3, but Polycose sensitivity remains relatively normal. *American journal of physiology Regulatory, integrative and comparative physiology* 303: R218-235, 2012.
46. **Valenzuela FJ, Vera J, Venegas C, Munoz S, Oyarce S, Munoz K, and Lagunas C**. Evidences of Polymorphism Associated with Circadian System and Risk of Pathologies: A Review of the Literature. *International journal of endocrinology* 2016: 2746909, 2016.
47. **Yee KK, Sukumaran SK, Kotha R, Gilbertson TA, and Margolskee RF**. Glucose transporters and ATP-gated K+ (KATP) metabolic sensors are present in type 1 taste receptor 3 (T1r3)-expressing taste cells. *Proceedings of the National Academy of Sciences of the United States of America* 108: 5431-5436, 2011.
48. **Yin X, Li Y, Xu G, An W, and Zhang W**. Ghrelin fluctuation, what determines its production? *Acta biochimica et biophysica Sinica* 41: 188-197, 2009.
49. **Yoshikawa T, Inoue R, Matsumoto M, Yajima T, Ushida K, and Iwanaga T**. Comparative expression of hexose transporters (SGLT1, GLUT1, GLUT2 and GLUT5) throughout the mouse gastrointestinal tract. *Histochemistry and cell biology* 135: 183-194, 2011.
50. **Zhao GQ, Zhang Y, Hoon MA, Chandrashekar J, Erlenbach I, Ryba NJ, and Zuker CS**. The receptors for mammalian sweet and umami taste. *Cell* 115: 255-266, 2003.
51. **Zhao X, Cho H, Yu RT, Atkins AR, Downes M, and Evans RM**. Nuclear receptors rock around the clock. *EMBO reports* 15: 518-528, 2014.

586

587

588 Figure legends

589 Figure 1 Small intestinal hexose transporter mRNA expression levels in the morning and evening. Whole
590 duodenum, jejunum and ileum was dissected from six-week-old CD-1 mice at 7am or 7pm (n=8 per
591 group) for subsequent quantitative PCR of *slc5a1* (SGLT1), *slc2a2* (GLUT2) and *slc2a5* (GLUT5). Values
592 were normalised against 3 reference genes and relative quantitation was performed using the ddCT
593 method and are expressed relative to duodenum at 7am. *P < 0.05, **P < 0.01, ***P < 0.001, ns = not
594 significant.

595

596 Figure 2 Small intestinal GLUT2 protein expression levels in the morning and evening. Whole duodenum,
597 jejunum and ileum was dissected from ten-week-old C57BL/6 mice (n=8 per group) for subsequent
598 protein extraction and Western blots of βActin and GLUT2. Representative blots are shown. Blots were
599 quantified and normalised against βActin and are expressed relative to 7am. *P < 0.05, **P < 0.01, ***P
600 < 0.001, ns = not significant.

601

602 Figure 3 Nutrient sensor mRNA expression levels along the length of the murine alimentary tract in the
603 morning and evening. Whole tongue, stomach, duodenum, jejunum and ileum was dissected from six-
604 week old CD-1 mice at 7am or 7pm (n=8 per group) and total RNA isolated for subsequent quantitative
605 PCR of *tas1r1* (T1R1), *tas1r2* (T1R2), *tas1r3* (T1R3), *gnat1* (αTransducin) and *gnat3* (αGustducin). Values
606 are normalised against 3 reference genes and relative quantitation performed using the ddCT method
607 and expressed relative to duodenum at 7am. *P < 0.05, **P < 0.01, ***P < 0.001, ns = not significant. nd
608 = not detected

609

610

611 Figure 4 SGLT3a and SGLT3b mRNA expression levels along the length of the murine alimentary tract in
612 the morning and evening. Whole tongue, stomach, duodenum, jejunum and ileum was dissected from
613 six-week old CD-1 mice at 7am or 7pm (n=8 per group) and total RNA isolated for subsequent
614 quantitative PCR of *slc5a4a* (SGLT3a) and *slc5a4b* (SGLT3b). Values are normalised against 3 reference
615 genes and relative quantitation performed using the ddCT method and expressed relative to duodenum
616 at 7am. *P < 0.05, **P < 0.01, ***P < 0.001, ns = not significant. nd = not detected.

617

618

Figure 5 SGLT3 protein expression levels along the length of the murine alimentary tract in the morning and evening. Whole stomach, duodenum, jejunum and ileum was dissected from ten-week-old C57BL/6 mice (n=8 per group) for subsequent protein extraction and Western blots of βActin and SGLT3. Representative blots are shown. Blots were quantified, normalised against βActin and are expressed relative to 7am. *P < 0.05, **P < 0.01, ***P < 0.001, ns = not significant.

Figure 6 Gut peptide mRNA expression along the length of the murine alimentary tract in the morning and evening. Whole stomach, duodenum, jejunum and ileum was dissected from six-week-old CD-1 mice at 7am or 7pm (n=8 per group) and total RNA isolated for subsequent quantitative PCR of *cck* (CCK), *gip* (GIP), *gcg* (Preproglucagon) and *ghrl* (Ghrelin). Values are normalised against 3 reference genes and relative quantitation performed using the ddCT method and expressed relative to duodenum at 7am. *P < 0.05, **P < 0.01, ***P < 0.001, ns = not significant.

Figure 7 Clock gene mRNA expression levels along the length of the murine alimentary tract in the morning and evening. Whole tongue, stomach, duodenum, jejunum and ileum was dissected from six-week old CD-1 mice (n=8 per group) and total RNA isolated for subsequent quantitative PCR of *cry2* (CRY2) and *arntl1* (BMAL1). Values are normalised against 3 reference genes and relative quantitation performed using the ddCT method and expressed relative to duodenum at 7am. *P < 0.05, **P < 0.01, ***P < 0.001, ns = not significant.

Table 1 Fold changes of diurnally regulated gut peptides in the murine tongue. Total RNA obtained from CD-1 mice tongue at 7 am (n=8) and 7pm (n=8) was pooled and analysed on an Affymetrix microarray chip.

Table 2 *In silico* promotor analysis of hexose transporters and nutrient sensor genes for sequences of diurnal E-Box elements. 10,000bp upstream of each translation start were used to find E-Box sequences and matching extended consensus sequences are marked in bold.

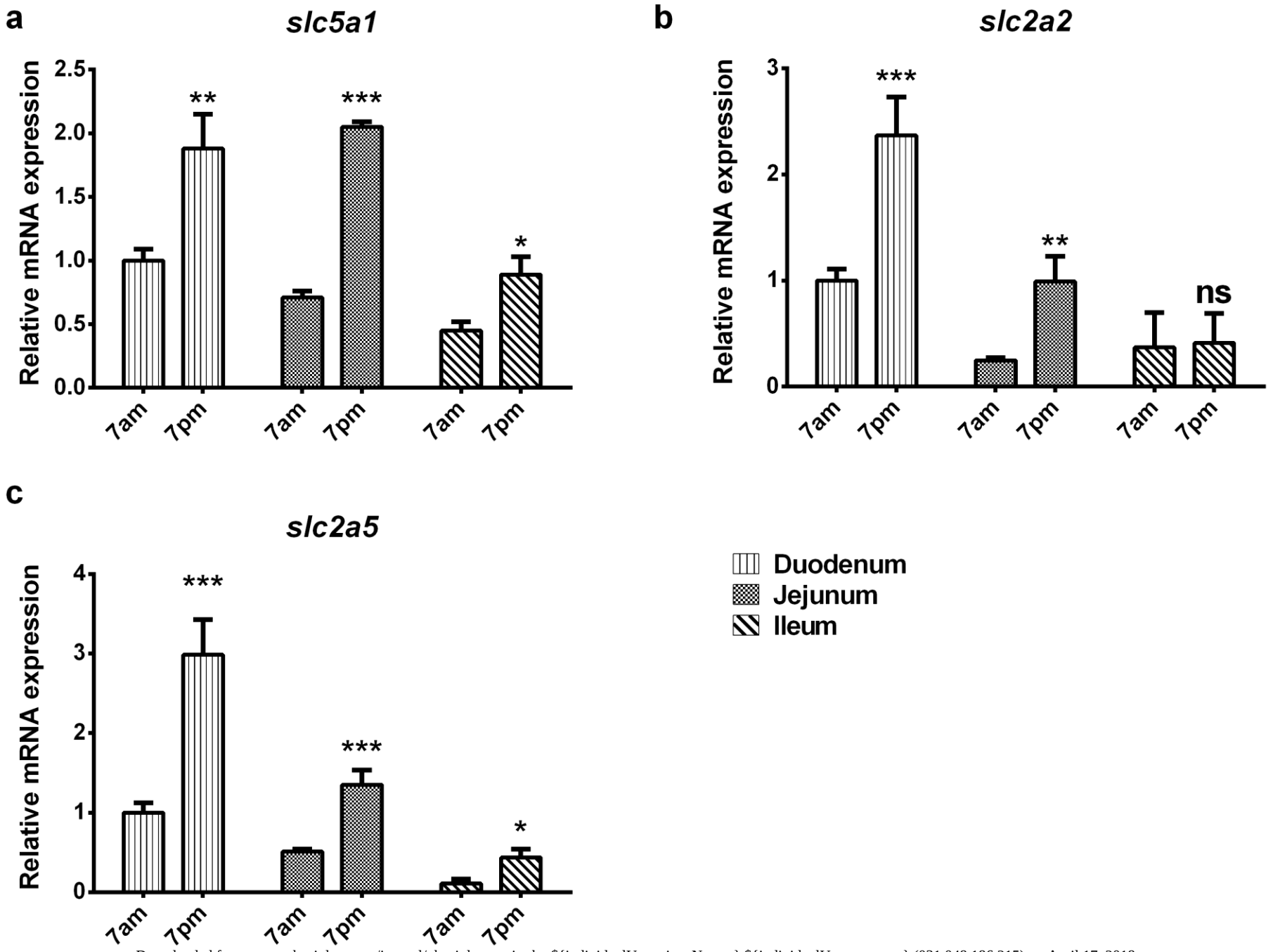

Fig 1

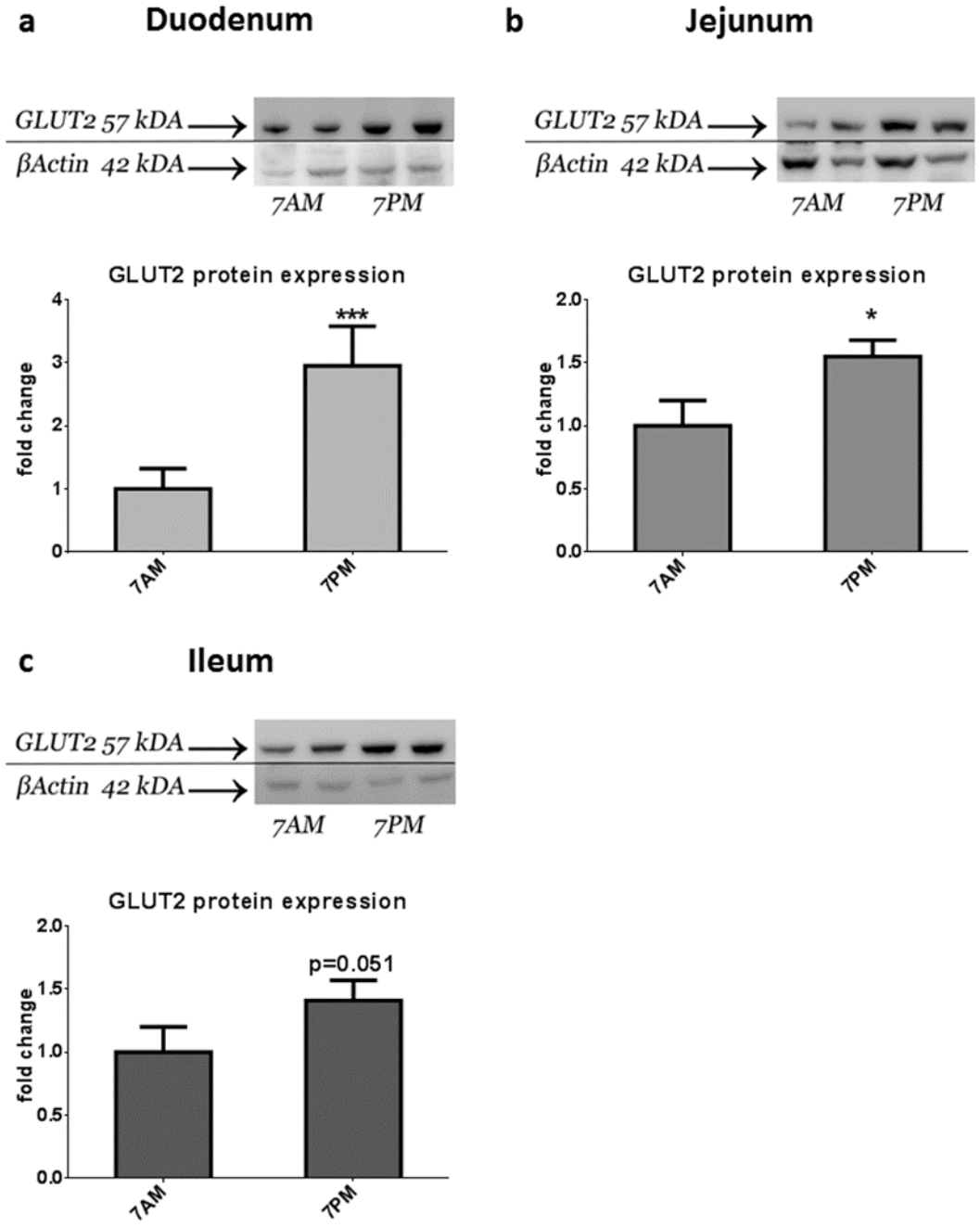

Fig 2

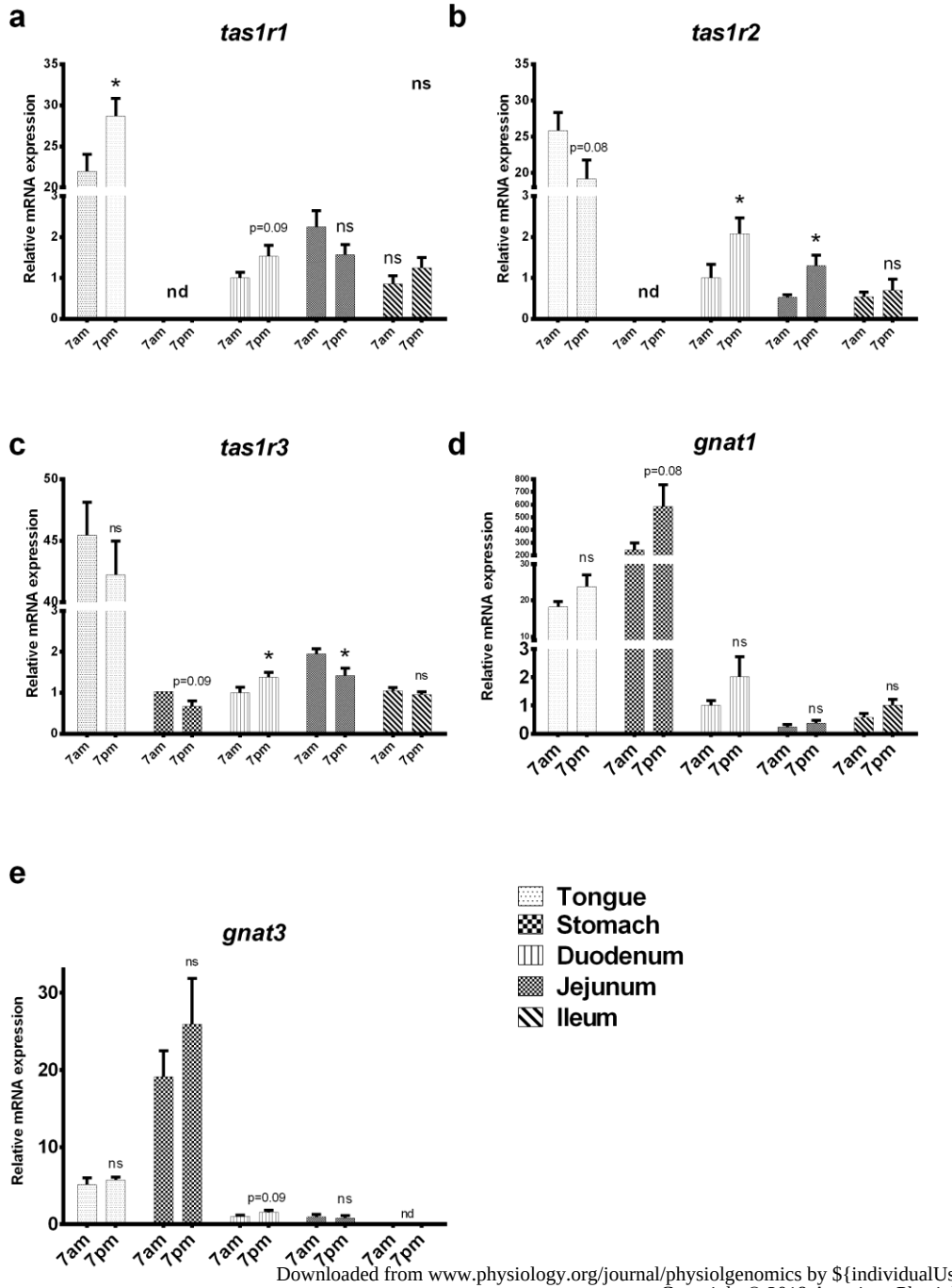

Fig 3

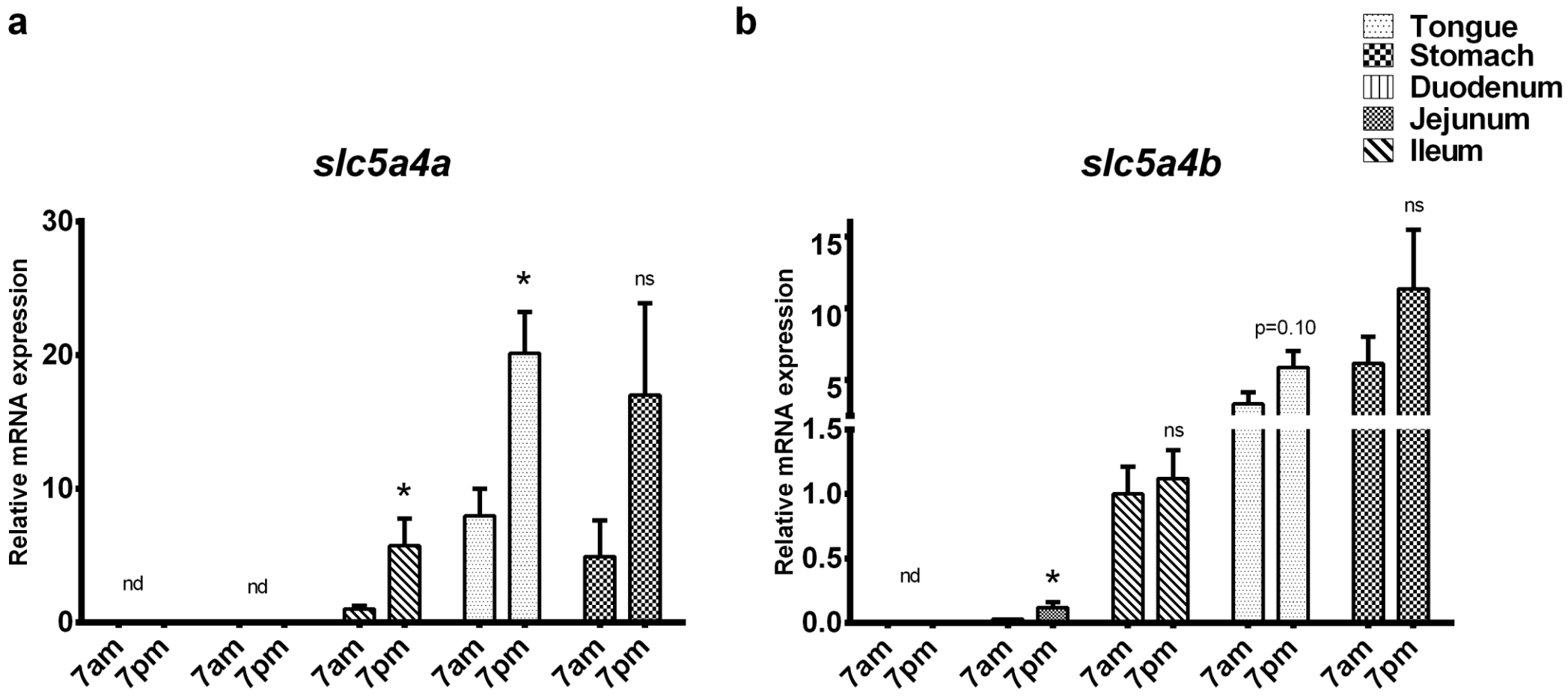

Fig 4

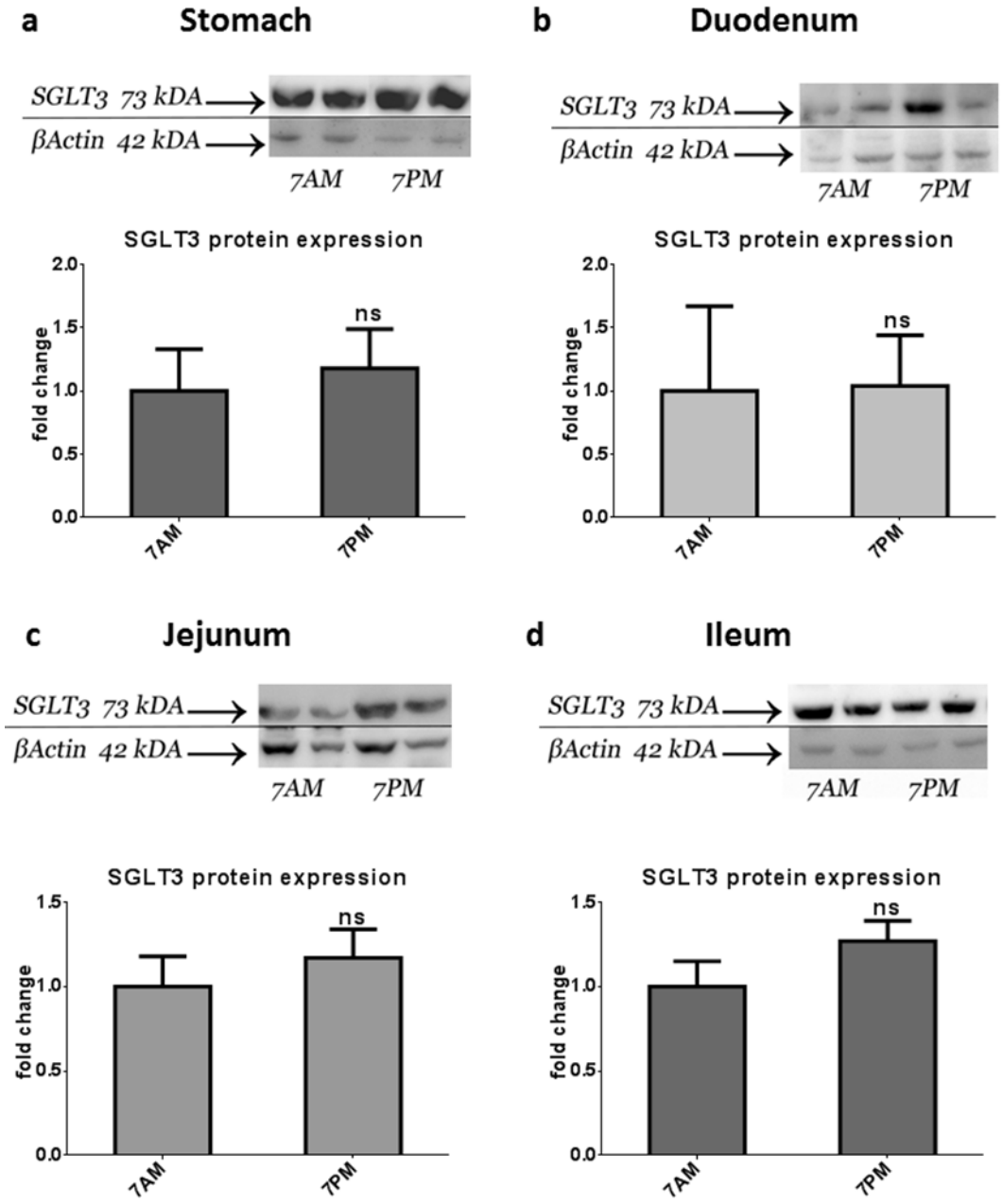

Fig 5

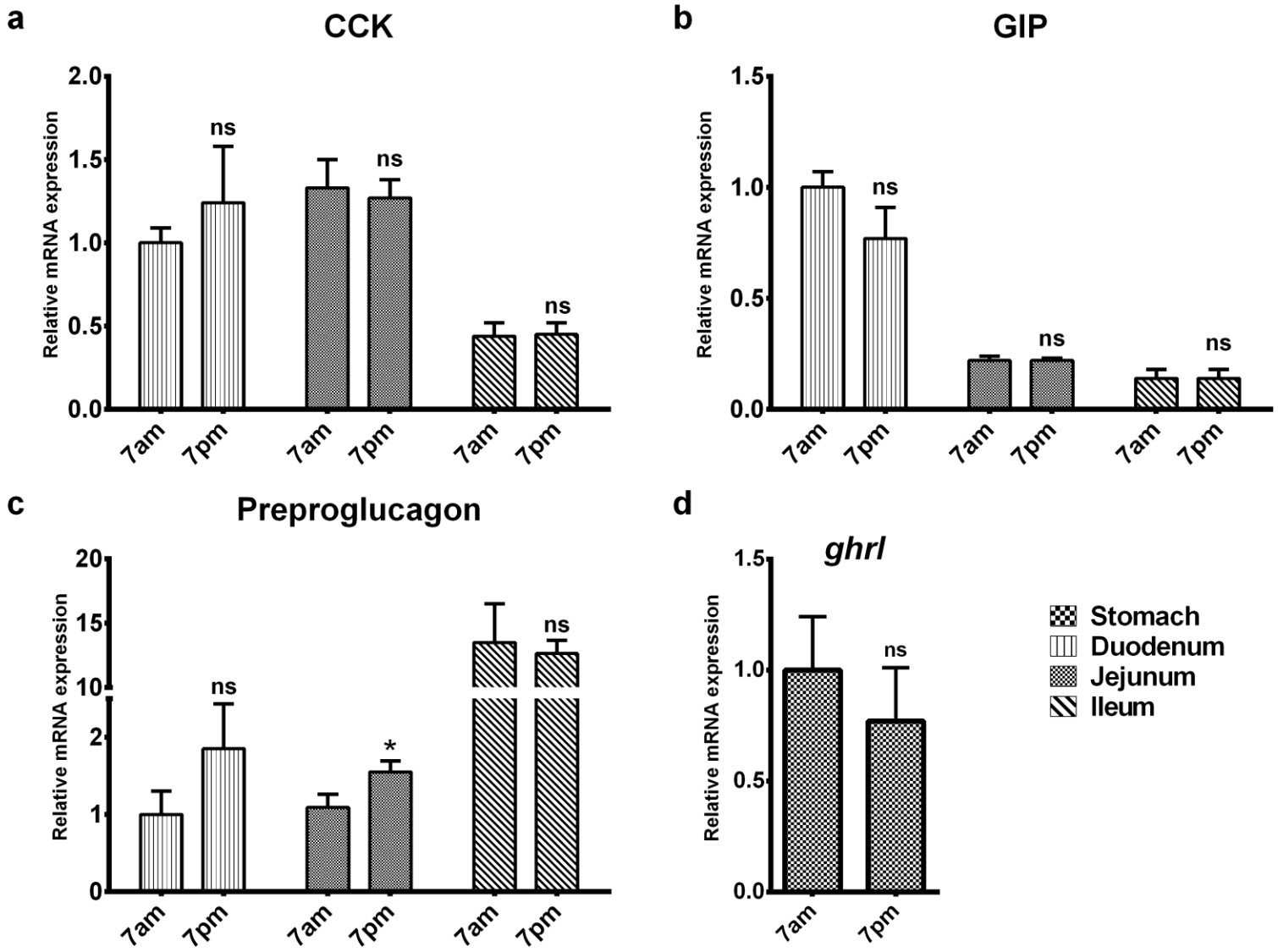

Fig 6

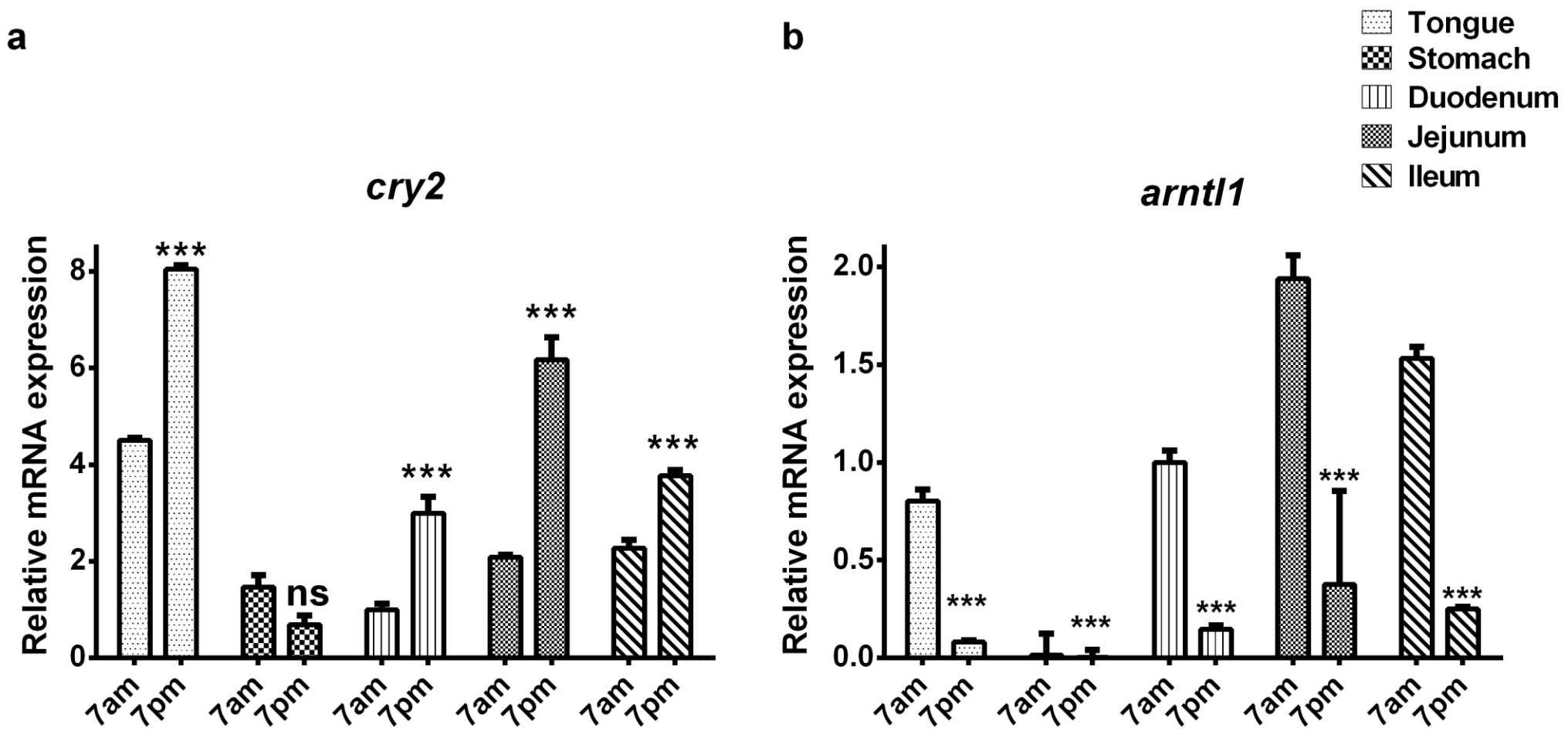

Fig 7

Diurnal regulation of gut peptides in mouse tongue

Protein	Gene name	Fold change 7am vs 7pm
Preproglucagon	*gcg*	-3.23
GIP	*gip*	2.12
PYY	*pyy*	-1.90
Ghrelin	*ghrl*	-2.65
CCK	*cck*	-1.61

Table 1

E-Box elements in 10,000 bp upstream region of genes

	-7	-6	-5	-4	Consensus	+4	+5	+6	+7
Gene name	G/T	G	A/G	A	CACGTG	A	C	C	C
arntl1	T	G	G	A	CACGTG	C	C	C	G
cry2					X				
slc5a1	G	C	C	T	CACGTG	G	G	A	C
slc2a2	T	G	G	A	CACGTG	A	G	C	C
tas1r1	C	C	G	C	CACGTG	C	G	C	G
tas1r2	C	A	T	T	CACGTG	G	C	C	C
tas1r3	C	A	G	A	CACGTG	C	T	C	C
slc5a4a	C	C	A	A	CACGTG	T	C	T	T
slc5a4b	G	A	G	C	CACGTG	T	T	C	T
ghrl	T	A	C	A	CACGTG	G	A	A	A
gip					X				
cck	T	G	A	G	CACGTG	T	C	C	T
gcg					X				
pyy	T	C	C	T	CACGTG	T	G	C	T

Table 2